0031-3998/10/6704-0345
PEDIATRIC RESEARCH

Vol. 67, No. 4, 2010
Printed in U.S.A.

Macrophages Are Targeted by Rotavirus in Experimental Biliary Atresia and Induce Neutrophil Chemotaxis by Mip2/Cxcl2

SUJIT K. MOHANTY, CLÁUDIA A. P. IVANTES, REENA MOURYA, CRISTINA PACHECO, AND JORGE A. BEZERRA

Cincinnati Children's Hospital Medical Center and the Department of Pediatrics [S.K.M., R.M., J.A.B.], University of Cincinnati College of Medicine, Cincinnati, Ohio 45229; Department of Internal Medicine [C.A.P.I.], Federal University of Paraná, Curitiba, PR, 80045-070 Brazil; Department of Pathology [C.P.], Children's Hospitals and Clinics of Minnesota, Minneapolis, Minnesota 55404

ABSTRACT: Biliary atresia is an obstructive cholangiopathy of unknown etiology. Although the adaptive immune system has been shown to regulate the obstruction of bile ducts in a rotavirus-induced mouse model, little is known about the virus-induced inflammatory response. Here, we hypothesized that cholangiocytes secrete chemoattractants in response to rotavirus. To test this hypothesis, we infected cholangiocyte and macrophage cell lines with rhesus rotavirus type A (RRV), quantified cytokines and chemokines and measured the migration of splenocytes. We also used PCR and immunostaining to search for new cellular targets of RRV in the liver. We found that RRV-infected cholangiocytes induced the mRNA expression for chemokines, but conditioned media failed to promote chemotaxis of splenocytes. Analyzing livers after viral challenge, we detected RRV in hepatic macrophages and demonstrated that media from RRV-infected macrophages have high concentrations of cytokines and chemokines and induced chemotaxis of neutrophils. Most notably, addition of anti-Mip2/Cxcl2 antibodies depleted this chemokine in the conditioned media and completely prevented neutrophil chemotaxis. In conclusion, infected cholangiocytes did not promote chemotaxis of inflammatory cells. Investigating alternate cellular targets of RRV, we detected the virus in hepatic macrophages and found that infected macrophages promoted neutrophil chemotaxis by release of Mip2/Cxcl2 in response to RRV. **(*Pediatr Res* 67: 345–351, 2010)**

Biliary atresia, the most common cause of neonatal cholestasis, results from an inflammatory and fibrosing obstruction of extrahepatic bile ducts. The etiology is unknown, but studies in an experimental mouse model of rotavirus-induced biliary atresia indicate that pathogenic mechanisms of disease begin with an injury to the biliary epithelium, followed by a robust inflammatory infiltration of the wall of extrahepatic bile ducts, obstruction of the lumen by inflammatory cells, and final progression to fibrosis (1). These pathologic changes in the liver and extrahepatic bile ducts closely resemble human biliary atresia (2,3). Studies of livers of infants at the time of diagnosis have long recognized an activation of inflammatory cells (4), and a broad analysis of the hepatic gene expression profile identified a prominent proinflammatory signature (5). Disruption of this signature by loss of IFN-γ or the loss of CD8+ lymphocytes in the mouse model largely prevented duct obstruction and the phenotype of experimental biliary atresia (6,7). Interestingly, *in vivo* depletion of CD4+ lymphocytes or the genetic loss of IL-12, or the depletion of TNF-α later in the course of biliary injury did not alter the progression to biliary atresia phenotype (7–9), which supported the coexistence of accessory pathways regulating the pathology of extrahepatic bile ducts. Despite the progress in deciphering key elements regulating duct obstruction and atresia, little is known about molecular circuits that are activated in early stages of the disease.

Cellular localization studies have shown that cholangiocytes are cellular targets in early stages of disease after rotavirus administration in newborn mice (6,10). This infection induces the creation of an environment rich in chemokines, some of which probably derive from cholangiocytes, as suggested by increased expression of monocyte chemotactic protein 1 (Mcp1), regulated on activation, normal T cell expressed and secreted (Rantes), KC/Cxcl1, macrophage inflammatory protein 2 (Mip2/Cxcl2), and thymus and activation regulated chemokine (Tarc) by a cholangiocyte cell line infected with rhesus rotavirus type A (RRV) (11). Further, when primary cholangiocytes were submitted to flow cytometry, they were reported to express the surface markers MHC I and II and CD40, but they did not function as competent antigen-presenting cells (12). Based on its role as a cellular target of RRV and as a source of inflammatory mediators, we hypothesized that cholangiocytes secrete chemoattractants to mononuclear cells in response to RRV. Testing this hypothesis, we found that conditioned media of RRV-infected cholangiocytes did not induce chemotaxis to mononuclear cells. Exploring alternative cellular sources, we found that hepatic macrophages were targeted by RRV and that conditioned media from RRV-infected macrophages was rich in Mip2/Cxcl2, attracted neutrophils, and lost chemoattractant properties after depletion of Mip2/Cxcl2.

METHODS

Cell culture and viral infection. The murine cholangiocyte cell line mCL, a SV40-large T-antigen–transformed cell from Balb/c mice (13), was cultured

Received August 21, 2009; accepted December 4, 2009.

Correspondence: Jorge A. Bezerra, M.D., Cincinnati Children's Hospital Medical Center, 3333 Burnet Avenue, Cincinnati, OH 45229-3039; e-mail: jorge.bezerra@cchmc.org

This work was supported by funding from the National Institutes of Health, grant number DK064008 [J.A.B.] and grant number DK078392, to the Integrative Morphology Core of the Digestive Disease Research Core Center at Cincinnati Children's Hospital Medical Center.

S.K.M. and C.A.P.I. contributed equally to the work.

Abbreviations: Mip2, macrophage inflammatory protein 2; **RRV,** rhesus rotavirus type A

in DMEM (Cellgro, Herndon, VA) containing 10% heat-inactivated fetal bovine serum, 100 U/mL penicillin, 100 μg/mL streptomycin (Invitrogen, Carlsbad, CA), and 1% L-glutamine (Invitrogen) at 37°C in 5% CO_2-humidified air. Raw 264.7 cells were obtained from American Type Culture Collection (Manassas, VA) and cultured under the conditions described in the protocol PP0159 of the Alliance for Cellular Signaling (www.signaling-gateway.org). For viral infection, mCL and Raw 264.7 cells were plated in a 12-well dish at a density of 0.2×10^6 (for mCL) or 0.5×10^6 (for Raw 264.7) cells/well. After 2 d of culture, cells were washed twice and cultured for 1 h in Earle's Balanced Salt Solution-Ca^{++} (EBSS, Sigma Chemical Co.-Aldrich, St. Louis, MO) with 4 μg/mL of trypsin containing live virus at a multiplicity of infection of 100 to ensure high infection rate of plated cells. Cultured cells were then washed twice, and further incubated in serum-free DMEM for variable intervals. At defined time points, the conditioned medium was aspirated and stored at −20°C until the time of analysis and cells were used for RNA isolation. For chemotaxis assays, the conditioned medium was transferred freshly from the culture wells to the chemotaxis chambers.

Chemotaxis assay. Wedge chemotactic response was based on 48-well microchemotaxis chamber (Neuro Probe, Gaithersburg, MD) as described previously (14). In brief, the lower well contained 27 μL of conditioned media from RRV-infected or naïve mCL or Raw 264.7 cells. The upper chamber was filled with 50 μL of splenocytes or neutrophils (final concentration of 2×10^6 cells per mL) isolated from normal adult Balb/c mice. The well and chamber were separated by a 3.0-μm pore size polycarbonate filter. The assay chambers were incubated at 37°C in 5% CO_2 for 45 min at which time the chambers were disassembled, the membranes were washed, fixed in methanol, and stained with Diff-Quick staining kit (Fisher Scientific, Pittsburgh, PA). The cells on the inferior surface of the membranes were counted from five fields of each membrane at 400× magnification using a Nikon Labophot 2 Microscope (Nikon, Melville, NY), and the mean cell number was calculated for individual wells; each experiment was performed in quadruplicate. fMLP 1 μM (Sigma Chemical Co.-Aldrich) was added to separate wells as a positive control. All experiments were repeated two to three times unless otherwise stated, and the results are expressed as mean cells/high-power field ± SE.

Animal model and cell isolation. Balb/c mice were injected with 0.9% saline solution (controls) or 1.5×10^6 focus-forming units (ffu) of RRV intraperitoneally within 24 h of birth. Each group of RRV- or saline-injected mice contained three to five newborn mice per time point, unless otherwise specified in the results or in figure legends. All mice were examined daily and the diagnosis of experimental biliary atresia was determined by the presence of jaundice in non–fur-covered skin and acholic stools, as well as by the direct finding of luminal obstruction in serial sections of extrahepatic bile ducts harvested at 7 or 14 d after RRV infection and stained with hematoxylin-eosin, as described by us in a previous publication (6); the phenotype cannot be ascertained 3 d after RRV infection because the first signs of cholestasis emerge at d 5 and 6. At the time of sacrifice, livers were snap frozen in liquid N_2 for analysis of mRNA expression or used for isolation of mononuclear cells as described previously with minor modifications (8). In brief, livers were minced, passed through a nylon mesh, layered on 3 mL of histopaque (Sigma Chemical Co.), and centrifuged at 270 × g. Freshly isolated mononuclear cells were used in immunofluorescence assays or processed for RNA isolation (see later). The Institutional Animal Care and Use Committee of the Cincinnati Children's Research Foundation approved all animal protocols.

Immunofluorescence assay. For immunofluorescence, primary liver suspensions of mononuclear cells obtained 7 d after RRV infection were centrifuged, the supernatant was removed, and the cell pellet was cytospun onto a glass slide, fixed in cold 80% acetone for 10 min, and then in cold methanol for 10 min. Fixed cells were blocked with 2% normal goat serum, incubated with anti-rotavirus and anti-F4/80 primary antibodies overnight at 4°C, washed, and then incubated with Texas red- and FITC-conjugated secondary antibodies. The cells/slides were washed twice and mounted using permount/DAPI.

Chemokine and cytokine ELISAs. The concentration of chemokines and cytokines was determined in conditioned media using commercially available ELISA Quantikine sandwich enzyme immunoassay kits for TNF-α, IFN-γ, IFN-α, IFN-β, IL-1β, Mip2/Cxcl2, and KC/Cxcl1 (R&D Systems, Minneapolis, MN), according to the manufacturer's instructions. A range of 50–100 μL of media was used for each well. The OD was determined using the Spectramax Plus microplate reader (Molecular Devices Corp, Sunnyvale, CA), and the concentration was calculated with the Softmax Pro v2.2.1 software (Molecular Devices Corp).

Chemokine immunodepletion. Mip2/Cxcl2 was depleted from conditioned media by incubation with 50 μg of mouse antibody against Mip2/Cxcl2 (R&D Systems) followed by incubation with CNBr-activated protein G sepharose overnight at 4°C, and washed to remove unbound products. Supernatants of RRV-infected or naïve macrophages in culture (1 mL of supernatant collected after 12 h of culture) were incubated with the protein G-coupled antibody mixture and incubated for 2 h at room temperature. Immune complexes were pelleted at 2500 × g for 3 min and the supernatant was collected for chemotaxis assay. The immunodepletion protocol was also applied to supernatants without anti-Mip2/Cxcl2 antibody to serve as controls. The efficiency of Mip2/Cxcl2 immunodepletion was determined by ELISA (as described above) by measuring the concentration of the chemokine in supernatants before and after immunodepletion.

Real-time PCR. RNA from the whole liver and mCL cells was isolated using Trizol (Invitrogen), reverse transcribed with the MMLV reverse-transcription kit from Invitrogen, and subjected to real-time PCR in a Mx3000P (Stratagene, LA Jolla, CA) as described previously (6,7) using specific primers for individual genes (Table 1).

Statistical analysis. Values are expressed as mean ± SE and statistical significance was determined by two-tailed, unpaired *t* test, with a significance set at $p < 0.05$. Numbers of samples for individual experiments are described in the results or figure legends.

Table 1. *Oligonucleotide primers used for detection of different chemokines*

Gene	Primer sequences	Annealing temperature (°C)
KC/Cxcl1	Forward: 5′-ACCGAAGTCATAGCCACACTC-3′ Reverse: 5′-TGGGGACACCTTTTAGCATC-3′	52
Mip2/Cxcl2	Forward: 5′-CCCAGACAGAAGTCATAGCCAC-3′ Reverse: 5′-GCCTTGCCTTTGTTCAGTATC-3′	52
TNFα	Forward: 5′-AAGGGAGAGTGGTCAGTTGCC-3′ Reverse: 5′-CCTCAGGGAAGAGTCTGGAAAGG-3′	55
Rantes	Forward: 5′-GGAGTATTTCTACACCAGCAGC-3′ Reverse: 5′-TCTTGAACCCACTTCTTCTCTG-3′	52
Cxcl9	Forward: 5′-GAGCTAGATAGACCTCACCAAG-3′ Reverse: 5′-CCATTAGCACCATCTCTGA-3′	55
Cxcl10	Forward: 5′-TCGCTCAAGTGGCTGGGATG-3′ Reverse: 5′-TAGGGAGGACAAGGAGGGTGTG-3′	55
Gapdh	Forward: 5′-TGGTTTGACAATGAATACGGCTAC-3′ Reverse: 5′-GGTGGGTGGTCCAAGGTTTC-3′	55
Rotavirus VP6	Forward: 5′-GCGGTAGCGGTGTTATTTCC-3′ Reverse: 5′-TTGTTTTGCTTGCGTCGG-3′	55
Rotavirus NSP3	Forward: 5′-TGTCAAGAGAATACCTGGGAAATC-3′ Reverse: 5′-GGAATCATCAACTTCAACTTCACC-3′	54
Ccl12	Forward: 5′-CACCATCAGTCCTCAGGTAT-3′ Reverse: 5′-GGACGTGAATCTTCTGCTTA-3′	54

RESULTS

RRV infection induces the expression of chemokines by cholangiocytes. We have shown that RRV infects and replicates in biliary epithelial cells (6). To determine whether the infection induces the expression of soluble mediators that localize the inflammatory response to the duct epithelium, we quantified the mRNA expression of chemokines known to be important to the recruitment of neutrophils (*Mip2/Cxcl2* and *KC/Cxcl1*) and T and NK cells (*Rantes, Cxcl9, Cxcl10, Ccl12*) after RRV infection of a cholangiocyte cell line from Balb/c mice (15–17). We found that RRV infection of cholangiocytes induces the expression of all chemokines several fold above RRV-naïve cholangiocytes (Fig. 1). mRNA expression was uniformly higher at or beyond 6 h of culture for all chemokines, with *KC/Cxcl1* and *Rantes* mRNA also increasing as early as 1 h after RRV challenge. Based on these data and on a previous report that these chemokines are also expressed at the protein level after RRV infection of mCL cells (11), we determined the ability of conditioned media to induce chemotaxis to splenocytes. To our surprise, conditioned media obtained after 12 and 24 h of culture did not attract splenocytes after 15, 30, or 45 min of culture despite the expression of chemokines, whereas many splenocytes migrated through the interchamber membrane toward fMLP as a positive control (data not shown). Therefore, we explored the existence of other cellular targets of RRV that could play a role in the production of soluble chemoattractants.

Hepatic macrophages are targeted by RRV. To examine whether liver nonepithelial cells are targeted by RRV in experimental biliary atresia, we isolated hepatic mononuclear cells by histopaque gradient at 3, 7, and 14 d after injection of RRV into Balb/c newborn mice within 24 h of birth. Mice were asymptomatic 3 d after infection but displayed jaundice and had acholic stools at 7 and 14 d, as reported previously (6). Using RNA from the hepatic mononuclear cells, we detected mRNA encoding the viral proteins *NSP3* and *VP6* at all time points (Fig. 2*A*). Based on our previous report that hepatic lymphocytes do not express *NSP3* or *VP6* mRNA after RRV challenge (6,7), we subjected hepatic mononuclear cells isolated after 7 d of

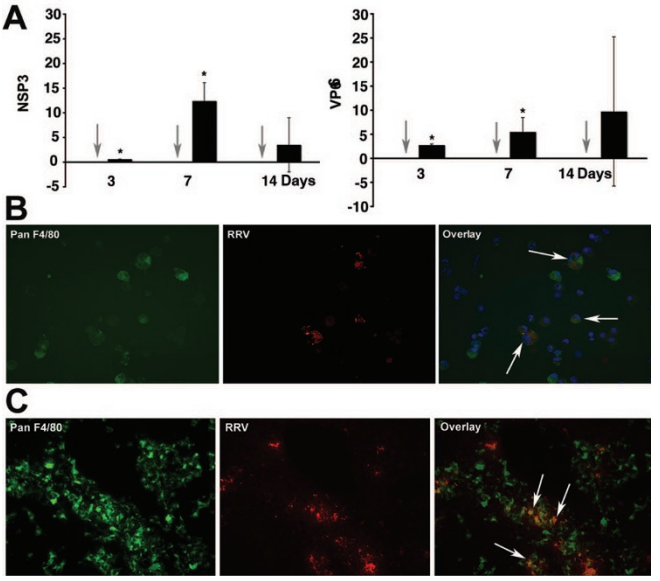

Figure 2. Detection of RRV in hepatic mononuclear cells and macrophages. *Panel A* depicts the expression of mRNA encoding for the RRV proteins *NSP3* and *VP6* in hepatic mononuclear cells isolated from mice 7 d after RRV challenge. Gray arrows point to no detection of RRV in hepatic mononuclear cells of normal saline-injected controls; black bars = RRV-injected mice; $p < 0.05$; $n = 3$–6 livers per time point and per experimental group. *Panels B and C* depict dual-immunofluorescence signals identifying RRV (red) in panF4/80+ cells (green) in purified hepatic mononuclear cells (*panel B*) or portal tracts (*panel C*) 7 d after RRV infection of newborn mice. Arrows point to double positive panF4/80+ and RRV+ cells.

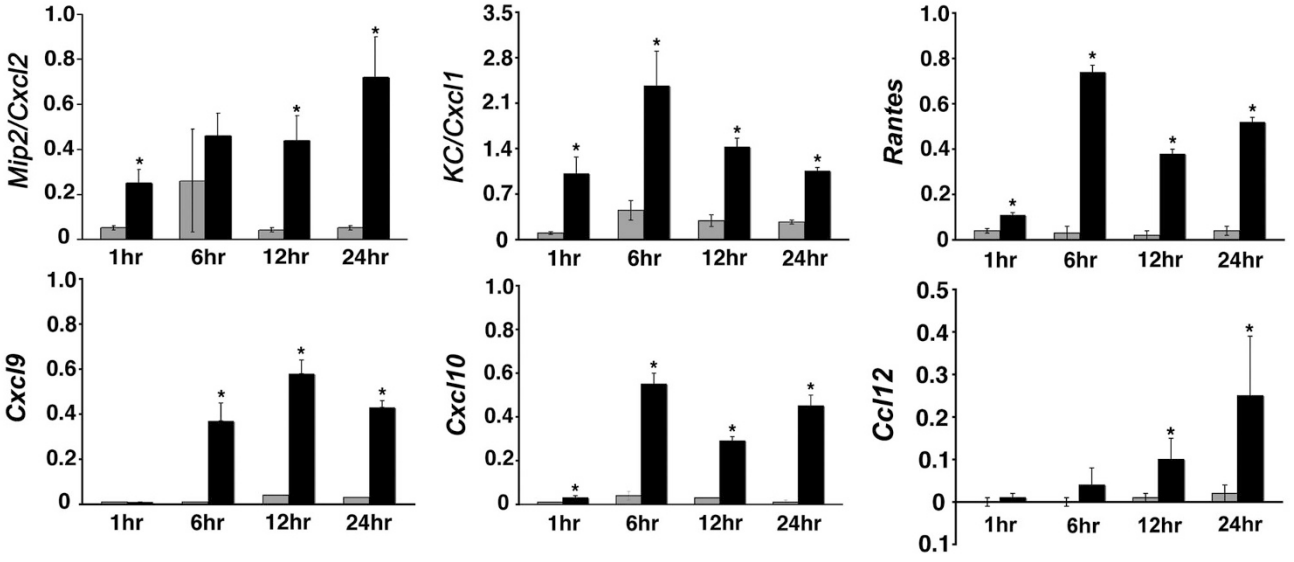

Figure 1. mRNA expression for chemokines by RRV-infected cholangiocytes. mRNA expression of chemokines in the cholangiocyte line mCL in culture at different time points after infection with RRV. mRNA levels were determined by real-time PCR and expressed as a ratio to *GAPDH*. *$p < 0.05$ (between RRV-infected and naïve mCL cells); gray bars = control (saline-injected mice); black bars = RRV-injected mice; $n = 3$ wells for each time point and experimental group.

infection to dual-fluorescence immunostaining using antibodies that identify macrophages (panF4/80) or RRV. We focused on panF4/80+ cells because macrophages from gut-associated lymphoid tissue have been previously reported to display rotavirus-specific proteins after oral challenge with rotavirus (18). We found that hepatic cells positive for panF4/80+ (macrophages) also stained positive for RRV (Fig. 2*B*). Consistent with the targeting of macrophages by RRV, immunostaining of liver sections 7 d after RRV infection detected panF4/80+ cells in portal spaces that also stained positive for RRV (Fig. 2*C*). Altogether, these data identify hepatic macrophages as nonparenchymal cells that are targeted by RRV in experimental biliary atresia.

Soluble mediators from RRV-infected macrophages induce chemotaxis of inflammatory cells. To investigate the role of macrophages as a source of chemoattractants after RRV infection, we made use of the macrophage cell line Raw 264.7. We did not use primary liver macrophages because of the very limited number of cells that can be isolated from very small neonatal livers. Further, Raw 264.7 cells have been used as a model system to study the biology of the rotavirus nonstructural protein NSP4 (19). In initial experiments, 1-h exposure of Raw 264.7 cells to RRV resulted in Raw cells staining positive for RRV after 24 h (Fig. 3*A*). Then, we collected conditioned media after 24 h of culture of RRV-infected and naïve Raw 264.7 cells and used them in chemotaxis assays. The presence of conditioned medium from RRV-infected Raw 264.7 cells induced migration of neutrophils (and to a minor degree migration of lymphocytes) toward lower wells of chemotaxis chambers above the levels observed in chambers containing medium from RRV-naïve cells (Fig. 3*B*). These data demonstrated that soluble mediators of chemotaxis are released from macrophages after RRV challenge and formed a suitable experimental system to search for key inducers of chemotaxis.

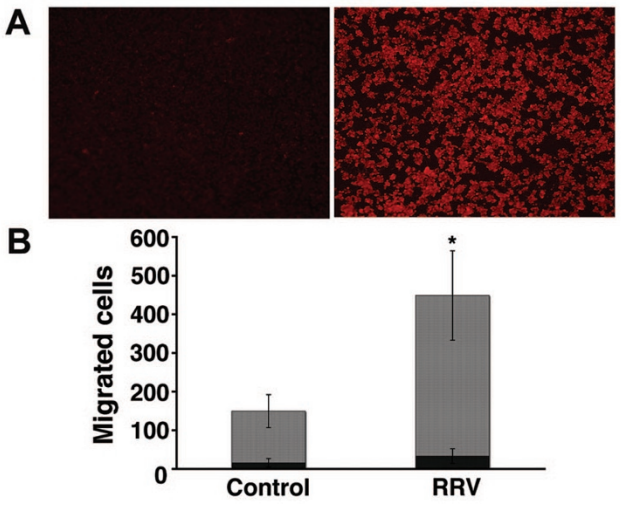

Figure 3. RRV infection of Raw 264.7 cells and induction of chemotaxis by conditioned media. In *panel A*, immunofluorescence detects RRV (*red* signal) 24 h after Raw 264.7 cells were exposed to RRV (*right photograph*); no signal is detected in cells not exposed to RRV (*left photograph*). *Panel B* depicts the numbers of neutrophils and lymphocytes that migrated to lower wells of chemotaxis chambers containing conditioned media from RRV-infected or control (RRV-naïve) Raw 264.7 cells after 45 min of culture. *$p < 0.05$; $n = 3$ chambers per group; gray bars = neutrophils; black bars = lymphocytes.

Table 2. *Presence or absence of protein levels of cytokines and chemokines in conditioned media obtained after 24 h of culture of RRV-infected Raw 264.7 and mCL cells*

Protein	mCL cells	Raw 264.7 cells
TNFα	—	+
IFNγ	—	—
IFNα	—	+
IFNβ	—	+
IL1β	—	—
Mip2/Cxcl2	+	+
KC/Cxcl1	+	—

Protein levels were determined by ELISA.
—, not detectable.

Macrophage-derived Mip2/Cxcl2 induces migration of neutrophils. Because cholangiocyte media did not induce chemotaxis despite the mRNA expression for chemokines, we determined the concentration of proinflammatory cytokines (TNF-α, IFN-γ, IFN-α, IFN-β, and IL-1β) and selected chemokines (Mip2/Cxcl2 and KC/Cxcl1) in media from Raw 264.7 cells and cholangiocytes. We found prominent increases in TNF-α, IFN-α, IFN-β, and Mip2/Cxcl2 primarily in macrophages, with undetectable levels for TNF-α, IFNγ, IFN-α, IFN-β, and IL-1β in media from cholangiocytes (Table 2 and Fig. 4). Of note, the concentration of Mip2/Cxcl2 in media from RRV-infected Raw 264.7 cells was 10-fold higher than in RRV-infected cholangiocytes at 24 h of culture (7130 ± 0.50 pg/mL *versus* 33 ± 1 pg/mL, respectively; $p < 0.01$). To examine whether the levels of Mip2/Cxcl2 increase during the development of experimental biliary atresia, we infected newborn mice with RRV and determined *Mip2/Cxcl2* mRNA expression by real-time PCR. We found that Mip2/Cxcl2 mRNA increases at early phases of injury (3 d after RRV challenge; $p < 0.05$) and remains variably elevated at the times of inflammatory obstruction (7 d) and atresia (14 d) of bile ducts (Fig. 5*A*). The significant increase in *Mip2/Cxcl2* mRNA at early phase of duct injury was temporally linked to the infiltration of neutrophils in portal tracts of RRV-infected mice (3 d; Fig. 5*B*), which differs from the predominantly lymphocytic infiltration at the time of duct obstruction (7 d; Fig. 5*B*). Combining these data with the well-established role of Mip2/Cxcl2 in chemotaxis of neutrophils (20), we hypothesized that macrophage-derived Mip2/Cxcl2 after RRV infection is a key inducer of chemotaxis.

To test this hypothesis, we performed new chemotaxis assays using conditioned media from RRV-infected and naïve Raw 264.7 cells that were depleted of Mip2/Cxcl2. Depletion was demonstrated by the undetectable level of Mip2/Cxcl2 by ELISA after incubation of conditioned media with anti-Mip2/Cxcl2 antibody (Fig. 6*A*). Use of Mip2/Cxcl2-depleted media in lower wells of chemotaxis chambers kept the number of migrated neutrophils at the same levels of conditioned media from RRV-naïve Raw 264.7 cells, whereas the Mip2/Cxcl2-containing media induced the typical surge in neutrophil migration (Fig. 6*B*).

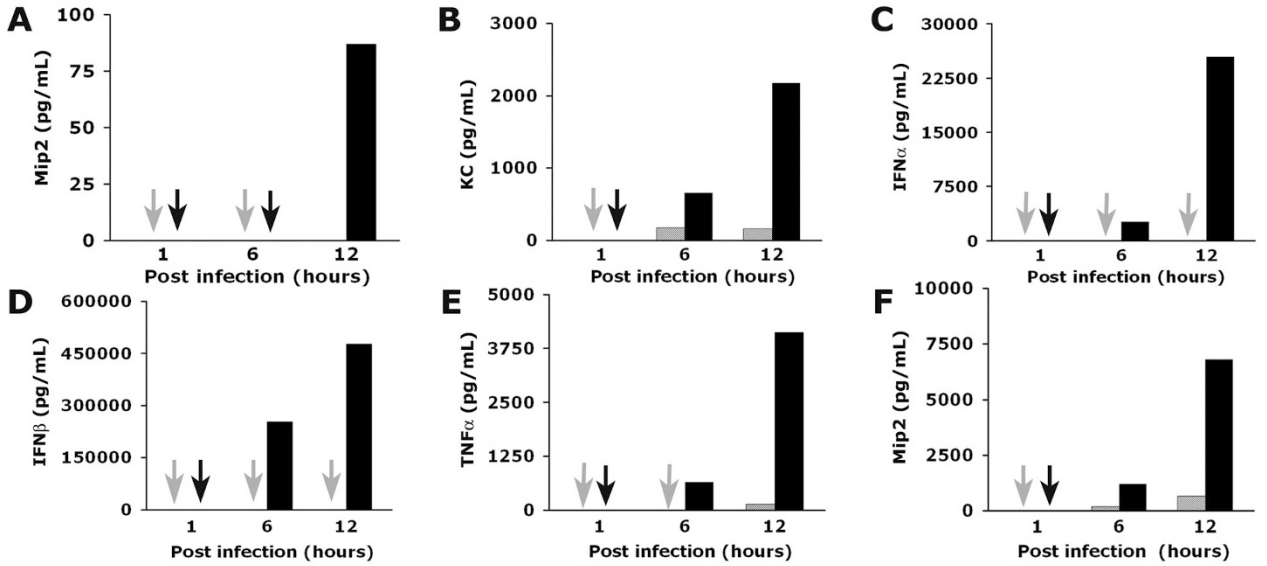

Figure 4. Production of cytokines and chemokines by mCL cholangiocytes and Raw 264.7 cells. Concentrations of cytokines and chemokines in conditioned media of RRV-infected and naïve (controls) mCL cholangiocytes (*panels A and B*) and Raw 264.7 (*panels C–F*) cells at different times of culture as determined by ELISA. Arrows point to no detectable level; $p < 0.05$ (between RRV-infected and naïve cells); gray bars = control (saline control cells); black bars = RRV-injected cells; $n = 3$ for each time point and experimental group.

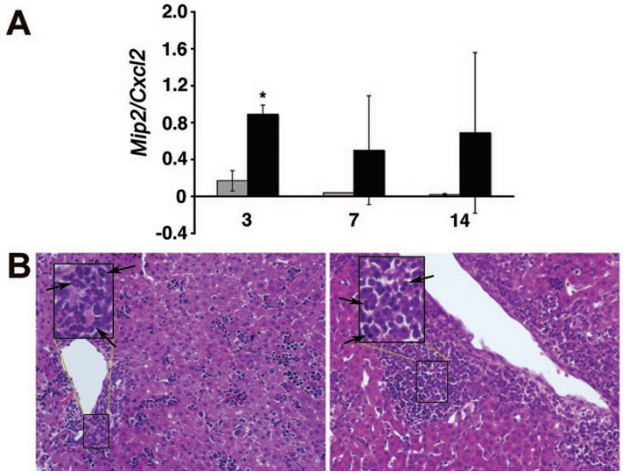

Figure 5. Hepatic expression of *Mip2/Cxcl2* and inflammation of portal tracts after RRV challenge. In *panel A*, real-time PCR shows increased hepatic expression of *Mip2/Cxcl2* mRNA 3 d after RRV infection of newborn mice; $p < 0.05$; gray bars = control (saline-injected mice); black bars = RRV-injected mice; $n = 3$ at each time point and experimental group. In *panel B*, hematoxylin/eosin staining of liver sections shows accumulation of neutrophils at d 3 (*arrows*; *left panel*) and lymphocytes at d 7 (*arrows; right panel*) after RRV infection. Insets represent magnification of area within rectangles; magnification: ×400.

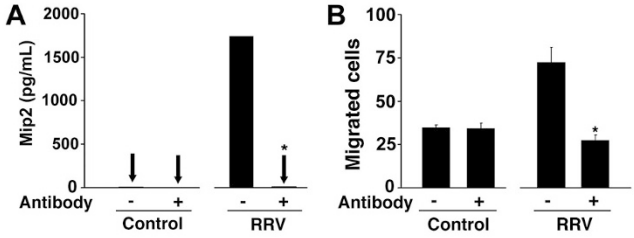

Figure 6. Mip2/Cxcl2-dependent chemotaxis of neutrophils. In *panel A*, the concentration of Mip2/Cxcl2 is determined in conditioned media from RRV-infected or RRV-naïve Raw 264.7 cells that were incubated (or not) with anti-Mip2/Cxcl2 antibody. *Panel B* depicts the number of neutrophils migrating to the lower wells of chemotaxis chambers containing the respective conditioned media with or without anti-Mip2/Cxcl2 antibody. $*p < 0.05$ showing significant differences between media with or without preincubation with anti-Mip2/Cxcl2 antibody; $n = 3$ for each experimental group.

DISCUSSION

We found that macrophages, rather than cholangiocytes, produce chemoattractants in response to RRV infection. Using an *in vitro* infection system of a cholangiocyte cell line previously shown to be susceptible to RRV and to express an array of cytokines and chemokines (6,11,12), we did not find support for a direct role of these cells in the promotion of chemotaxis of inflammatory cells. Searching for other cells with potential role in the regulation of the inflammatory response in experimental biliary atresia, we detected RRV in hepatic mononuclear cells 3–14 d after infection and identified the virus in macrophages. Using the macrophage cell line Raw 264.7 to examine the role of these cells in production of chemoattractants to inflammatory cells, we found that they secrete proinflammatory cytokines previously linked to pathogenesis of biliary atresia [examples: IFN-γ and TNF-α (6,8,21)] and high levels of the chemokine Mip2/Cxcl2. Most notably, conditioned media from RRV-infected macrophages induced prominent migration of neutrophils, which was dependent on Mip2/Cxcl2. These data identify macrophages as a new cellular target of RRV in experimental biliary atresia and point to its role as a source of soluble mediators that amplify the inflammatory population of the hepatobiliary environment.

Cholangiocytes are key epithelial targets of RRV and undergo injury by hepatic NK and CD8+ cells during pathogenesis of experimental biliary atresia (6,7,10,22); hepatocytes are also susceptible to RRV but do so at a lower multiplicity of infection. The injury by inflammatory cells might relate to

the recognition of viral epitopes in infected cells and/or to aberrant expression of MHC-associated molecules. However, recent work by another laboratory showed that RRV-exposed cholangiocytes do not appear to function as antigen-presenting cells (12). Based on the findings of increased expression of chemokines by cholangiocytes, investigators have suggested that infected cells may play a role in immunomodulation (11,12). Addressing this scenario, we first found an increase in the mRNA expression for cytokines and chemokines, but the expression at the protein level was either below the detectable levels by ELISA (for TNF-α, IFN-α, INF-β, INF-γ, and IL-1β) or still very low when compared with the levels produced by the macrophage cell line (for Mip2). The reasons for the discrepancy between the levels of mRNA expression detected by real-time PCR and the protein levels are not obvious but may include the variable rates of translation of mRNA transcripts. Regardless of the cause for the discrepancies, we did not find support for the release of biologically sufficient amounts of chemoattractants to inflammatory cells by cholangiocytes. It is possible that the ongoing production of chemokines by cholangiocytes for expanded periods of time (beyond the 24 h investigated in our studies) could generate a higher concentration of chemoattractants. However, we chose to stay within the constraints of 24 h of infection to simulate early biologic events (*i.e.* periductal inflammation and cholangiocyte injury) induced in the model of experimental biliary atresia (6,23). The lack of support for a role of cholangiocytes in antigen presentation or as a source of chemoattractants does not negate the possibility that cholangiocytes are critical elements of the pathogenesis of biliary atresia. For example, RRV-harboring cholangiocytes are cellular targets of NK and CD8+ cells. Further, they must maintain mucosal continuity along the intra- and extrahepatic biliary tracts. When this continuity is disrupted by NK cell-mediated injury, duct damage occurs and the phenotype of experimental biliary atresia emerges over time. If NK cells are depleted *in vivo*, cholangiocyte injury is negligible and the atresia phenotype is prevented (22).

The detection of RRV proteins in hepatic macrophages expands the types of cells that are initially targeted by the virus in the neonatal liver and formally implicates the innate immune system in pathogenesis of experimental biliary atresia. It is possible that the RRV signal observed in hepatic macrophages represents viral antigens that have been processed and are being presented on the cell surface. If this is correct, macrophages may serve as antigen-presenting cells to induce an adaptive response targeted to bile ducts. Our data add an additional role for macrophages as producers of inflammatory mediators that recruit neutrophils to the site of infection. One of these mediators is Mip2/Cxcl2, as supported by the induction of Mip2/Cxcl2-dependent chemotaxis of neutrophils by conditioned media from RRV-infected Raw 264.7 cells and by the increased expression of Mip2/Cxcl2 mRNA in livers as early as 3 d after RRV infection. We do not know whether Mip2/Cxcl2-dependent chemoattraction of neutrophils is essential to the pathogenesis of bile duct injury *in vivo*, but the data reported herein form the basis for this line of future investigation.

Patient-based studies have implicated macrophages in pathogenesis of biliary atresia. The enriched expression of the lipopolysaccharide receptor CD14 in Kupffer cells and the population of the livers of children with biliary atresia by activated macrophages suggest that these cells contribute to the creation of a proinflammatory environment at diagnosis and/or after portoenterostomy (24,25). At least in one report, a greater population of macrophages in the affected liver was associated with poor outcome (25). Despite the lack of evidence of active viral infection at the time of diagnosis in most patients with biliary atresia, a previous exposure to viral proteins may be sufficient for the induction of proinflammatory signals. For example, the nonstructural protein 4 (NSP4) of RRV has been shown to trigger the expression of inducible nitric oxide synthase in ileal macrophages after RRV infection (19). Although the use of cell culture systems and the experimental model of rotavirus-induced biliary atresia in newborn mice are powerful tools to understand components of operative biologic processes, it is important to recognize that findings from either system require validation in tissues of affected children. Further dissection of the role of macrophages in pathogenesis of disease, either as an antigen-presenting cell or as one of the cellular targets of a viral insult, will also require the use of *in vitro* systems using human cells. This line of studies are likely to decipher how macrophages or macrophage-derived signals directly regulate mechanisms of disease and can be potential therapeutic targets to block progression of disease to end-stage cirrhosis.

Acknowledgments. We thank Dr. Pranavkumar Shivakumar for his expert assistance with chemotaxis assays and with the animal model of biliary atresia.

REFERENCES

1. Bezerra JA 2006 The next challenge in pediatric cholestasis: deciphering the pathogenesis of biliary atresia. J Pediatr Gastroenterol Nutr 43:S23–S29
2. Petersen C, Biermanns D, Kuske M, Schakel K, Meyer-Junghanel L, Mildenberger H 1997 New aspects in a murine model for extrahepatic biliary atresia. J Pediatr Surg 32:1190–1195
3. Riepenhoff-Talty M, Schaekel K, Clark HF, Mueller W, Uhnoo I, Rossi T, Fisher J, Ogra PL 1993 Group A rotaviruses produce extrahepatic biliary obstruction in orally inoculated newborn mice. Pediatr Res 33:394–399
4. Mack CL, Sokol RJ 2005 Unraveling the pathogenesis and etiology of biliary atresia. Pediatr Res 57:87R–94R
5. Bezerra JA, Tiao G, Ryckman FC, Alonso M, Sabla GE, Sneider B, Sokol RJ, Aronow BJ 2002 Genetic induction of proinflammatory immunity in children with biliary atresia. Lancet 360:1653–1659
6. Shivakumar P, Campbell KM, Sabla GE, Miethke A, Tiao G, McNeal MM, Ward RL, Bezerra JA 2004 Obstruction of extrahepatic bile ducts by lymphocytes is regulated by IFN-gamma in experimental biliary atresia. J Clin Invest 114:322–329
7. Shivakumar P, Sabla G, Mohanty S, McNeal M, Ward R, Stringer K, Caldwell C, Chougnet C, Bezerra JA 2007 Effector role of neonatal hepatic CD8+ lymphocytes in epithelial injury and autoimmunity in experimental biliary atresia. Gastroenterology 133:268–277
8. Mohanty SK, Shivakumar P, Sabla G, Bezerra JA 2006 Loss of interleukin-12 modifies the pro-inflammatory response but does not prevent duct obstruction in experimental biliary atresia. BMC Gastroenterol 6:14
9. Tucker RM, Hendrickson RJ, Mukaida N, Gill RG, Mack CL 2007 Progressive biliary destruction is independent of a functional tumor necrosis factor-alpha pathway in a rhesus rotavirus-induced murine model of biliary atresia. Viral Immunol 20:34–43
10. Allen SR, Jafri M, Donnelly B, McNeal M, Witte D, Bezerra J, Ward R, Tiao GM 2007 Effect of rotavirus strain on the murine model of biliary atresia. J Virol 81:1671–1679
11. Jafri M, Donnelly B, Bondoc A, Allen S, Tiao G 2009 Cholangiocyte secretion of chemokines in experimental biliary atresia. J Pediatr Surg 44:500–550
12. Barnes BH, Tucker RM, Wehrmann F, Mack DG, Ueno Y, Mack CL 2009 Cholangiocytes as immune modulators in rotavirus-induced murine biliary atresia. Liver Int 29:1253–1261

13. Mano Y, Ishii M, Kisara N, Kobayashi Y, Ueno Y, Kobayashi K, Hamada H, Toyota T 1998 Duct formation by immortalized mouse cholangiocytes: an in vitro model for cholangiopathies. Lab Invest 78:1467–1468
14. Filippi MD, Harris CE, Meller J, Gu Y, Zheng Y, Williams DA 2004 Localization of Rac2 via the C terminus and aspartic acid 150 specifies superoxide generation, actin polarity and chemotaxis in neutrophils. Nat Immunol 5:744–751
15. Loetscher P, Seitz M, Clark-Lewis I, Baggiolini M, Moser B 1996 Activation of NK cells by CC chemokines. Chemotaxis, Ca2+ mobilization, and enzyme release. J Immunol 156:322–327
16. Murphy WJ, Tian ZG, Asai O, Funakoshi S, Rotter P, Henry M, Strieter RM, Kunkel SL, Longo DL, Taub DD 1996 Chemokines and T lymphocyte activation: II. Facilitation of human T cell trafficking in severe combined immunodeficiency mice. J Immunol 156:2104–2111
17. Taub DD, Longo DL, Murphy WJ 1996 Human interferon-inducible protein-10 induces mononuclear cell infiltration in mice and promotes the migration of human T lymphocytes into the peripheral tissues and human peripheral blood lymphocytes-SCID mice. Blood 87:1423–1431
18. Brown KA, Offit PA 1998 Rotavirus-specific proteins are detected in murine macrophages in both intestinal and extraintestinal lymphoid tissues. Microb Pathog 24:327–331
19. Borghan MA, Mori Y, El-Mahmoudy AB, Ito N, Sugiyama M, Takewaki T, Minamoto N 2007 Induction of nitric oxide synthase by rotavirus enterotoxin NSP4: implication for rotavirus pathogenicity. J Gen Virol 88:2064–2072
20. Haskill S, Peace A, Morris J, Sporn SA, Anisowicz A, Lee SW, Smith T, Martin G, Ralph P, Sager R 1990 Identification of three related human GRO genes encoding cytokine functions. Proc Natl Acad Sci USA 87:7732–7736
21. Erickson N, Mohanty SK, Shivakumar P, Sabla G, Chakraborty R, Bezerra JA 2008 Temporal-spatial activation of apoptosis and epithelial injury in murine experimental biliary atresia. Hepatology 47:1567–1577
22. Shivakumar P, Sabla GE, Whitington P, Chougnet CA, Bezerra JA 2009 Neonatal NK cells target the mouse duct epithelium via Nkg2d and drive tissue-specific injury in experimental biliary atresia. J Clin Invest 119:2281–2290
23. Carvalho E, Liu C, Shivakumar P, Sabla G, Aronow B, Bezerra JA 2005 Analysis of the biliary transcriptome in experimental biliary atresia. Gastroenterology 129:713–717
24. Ahmed AF, Nio M, Ohtani H, Nagura H, Ohi R 2001 In situ CD14 expression in biliary atresia: comparison between early and late stages. J Pediatr Surg 36:240–243
25. Davenport M, Gonde C, Redkar R, Koukoulis G, Tredger M, Mieli-Vergani G, Portmann B, Howard ER 2001 Immunohistochemistry of the liver and biliary tree in extrahepatic biliary atresia. J Pediatr Surg 36:1017–1025